Inorg. Chem. **2005**, *44*, 9347–9352

New Metal–Organic Polygons Involving MM Quadruple Bonds: $M_8(O_2C^tBu)_4(\mu\text{-}SC_4H_2\text{-}3,4\text{-}\{CO_2\}_2)_6$ (M = Mo, W)

Matthew J. Byrnes, Malcolm H. Chisholm,* and Nathan J. Patmore

Department of Chemistry, The Ohio State University, 100 West 18th Avenue, Columbus, Ohio 43210-1185

Received September 5, 2005

The reactions between $M_2(O_2C^tBu)_4$, where M = Mo or W, and thienyl-3,4-dicarboxylic acid (0.5–1.5 equiv) in toluene proceed via a series of detectable intermediates to the compounds $M_8(O_2C^tBu)_4(\mu\text{-}SC_4H_2\text{-}3,4\text{-}\{CO_2\}_2)_6$, which are isolated as air-sensitive yellow (M = Mo) or red (M = W) powders and show parent molecular ions in their mass spectra (MALDI). The structure of the molybdenum complex was determined by single-crystal X-ray crystallography and shown to contain an unusual M_8 polygon involving four Mo_2 quadruply bonded units linked via the agency of the six 3,4-thienylcarboxylate groups. The structure has crystallographically imposed S_4 symmetry and may be described in terms of a highly distorted tetrahedron of Mo_2 units or a bisphenoid in which two Mo_2 units are linked by a thienyldicarboxylate such that intramolecular $Mo_2\cdots O$ bonding is present, while the other thienylcarboxylate bridges merely serve to link these two $[Mo_2]\cdots[Mo_2]$ units together. The color of the compounds arises from intense M_2 δ-to-thienyl π^* transitions and, in THF, the complexes are redox-active and show four successive quasi-reversible oxidation waves. The $[M_8]^+$ radical cations, generated by one-electron oxidation with $AgPF_6$, are shown to be valence-trapped (class II) by UV–vis–near-IR and electron paramagnetic resonance spectroscopy. These results are supported by the electronic structure calculations on model compounds $M_8(O_2CH)_4(\mu\text{-}SC_4H_2\text{-}3,4\text{-}\{CO\}_2)_6$ employing density functional theory that reveal only a small splitting of the M_2 δ manifold via mixing with the 3,4-thienylcarboxylate π system.

Introduction

Dicarboxylates have been used in the construction of numerous metal−organic frameworks[1] and metal−organic polygons, MOPs.[2] Yaghi et al. have outlined the principles by which the selection of the dicarboxylate linker can be used to determine the formation of specific nets or polygons.[3] A particularly exciting aspect of their work has been the design of structures with large cavities, which serve as porous solids for gas storage (H_2 and CH_4).[4] Cotton and co-workers have employed dinuclear units, specifically Mo_2^{4+}, Ru_2^{5+}, and Rh_2^{4+}, in the construction of molecular squares and triangles,[5] and recently Zhou et al. reported the synthesis of a Mo_{24}-containing polygon based on 12 Mo_2^{4+} units with an overall cube-octahedral symmetry by the use of isophthalate linkers, $C_6H_4\text{-}2,3\text{-}(CO_2)_2$.[6] In this laboratory, we have previously employed 2,5-thienylcarboxylates to form "dimers of dimers", and with the ter- and pentathienylcarboxylate linkers shown in **A** and **B**, we have obtained

* To whom correspondence should be addressed. E-mail: chisholm@chemistry.ohio-state.edu. Tel: 614-292-7216. Fax: 614-2929-0368.

(1) (a) Eddaoudi, M.; Moler, D. B.; Li, H.; Chen, B.; Reineke, T. M.; O'Keeffe, M.; Yaghi, O. M. *Acc. Chem. Res.* **2001**, *34*, 319. (b) Rosseinsky, M. J. *Microporous Mesoporous Mater.* **2004**, *73*, 15. (c) Rosi, N. L.; Kim, J.; Eddaoudi, M.; Chen, B.; O'Keeffe, M.; Yaghi, O. M. *J. Am. Chem. Soc.* **2005**, *127*, 1504. (d) Zou, R.-Q.; Jiang, L.; Senoh, H.; Takeichi, N.; Xu, Q. *Chem. Commun.* **2005**, 3526.

(2) (a) Moulton, B.; Lu, J.; Mondal, A.; Zaworotko, M. J. *Chem. Commun.* **2001**, 863. (b) Eddaoudi, M.; Kim, J.; Wachter, J. B.; Chae, H. K.; O'Keeffe, M.; Yaghi, O. M. *J. Am. Chem. Soc.* **2001**, *123*, 4368. (c) Sudik, A. C.; Millward, A. R.; Ockwig, N. W.; Cote, A. P.; Kim, J.; Yaghi, O. M. *J. Am. Chem. Soc.* **2005**, *127*, 7110.

(3) (a) Yaghi, O. M.; O'Keeffe, M.; Ockwig, N. W.; Chae, H. K.; Eddaoudi, M.; Kim, J. *Nature* **2003**, *423*, 705. (b) Ockwig, N. W.; Delgado-Friedrichs, O.; O'Keeffe, M.; Yaghi, O. M. *Acc. Chem. Res.* **2005**, *38*, 176.

(4) (a) Rowsell, J. L. C.; Yaghi, O. M. *Microporous Mesoporous Mater.* **2004**, *73*, 3. (b) Eddaoudi, M.; Kim, J.; Rosi, N.; Vodak, D.; Wachter, J. B.; O'Keeffe, M.; Yaghi, O. M. *Science* **2002**, *295*, 469. (c) Rowsell, J. L. C.; Millward, A. R.; Park, K. S.; Yaghi, O. M. *J. Am. Chem. Soc.* **2004**, *126*, 5666.

(5) (a) Cotton, F. A.; Lin, C.; Murillo, C. A. *Proc. Natl. Acad. Sci. U.S.A.* **2002**, *99*, 4810. (b) Cotton, F. A.; Lin, C.; Murillo, C. A. *Acc. Chem. Res.* **2001**, *34*, 759. (c) Angaridis, P.; Berry, J. F.; Cotton, F. A.; Murillo, C. A.; Wang, X. *J. Am. Chem. Soc.* **2003**, *125*, 10327.

(6) Ke, Y.; Collins, D. J.; Zhou, H.-C. *Inorg. Chem.* **2005**, *44*, 4154.

10.1021/ic051516s CCC: $30.25
Published on Web 11/11/2005

oligomers that represent a dynamic combinatorial library of species when present in solution due to the facility of carboxylate group scrambling.[7,8] Our early studies were prompted by the desire to study electronic coupling of the M_2 units for which the 2,5-thienyl substitution is favorable because of the M_2 δ-to-$O_2C-SC_4H_4-CO_2$ π^* interaction shown in **C**.

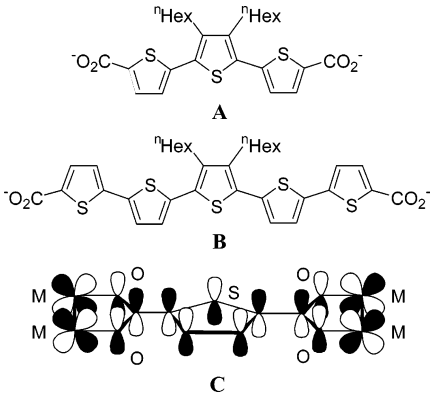

We were particularly interested to compare the electronic coupling and the molecular architecture that could be achieved by use of the 3,4-thienyldicarboxylate linker, which as seen in **D** might be expected to generate molecular loops and polygons.

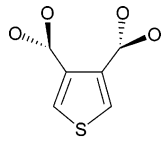

D

Experimental Section

Physical Procedures. UV−vis−near-IR spectra were recorded on a nitrogen-purged Perkin-Elmer Lambda 900 spectrometer. A 1.00-mm IR quartz cell was employed, and a spectrum of the neat solvent (THF) was subtracted. X-band EPR spectra (in THF) were recorded using a Bruker ESP300 electron spin resonance spectrometer. Temperature regulation was achieved using a Bruker variable-temperature unit. ^{1}H NMR spectra were recorded on a 400-MHz Bruker DPX Avance spectrometer and referenced to residual protio signals of THF-d_8 at $\delta = 3.58$.

Cyclic and differential pulse voltammograms were recorded at scan rates of 100 and 5 mV s^{-1}, respectively, under an inert atmosphere in a 0.1 M $^nBu_4NPF_6$/THF solution inside a single-compartment voltammetric cell equipped with a platinum working electrode, a platinum wire auxiliary electrode, and a pseudo reference electrode. Potential values were referenced to the $FeCp_2^{0/+}$ couple by the addition of a small amount of $FeCp_2$ to the solution.

Matrix-assisted laser desorption/ionization time of flight (MALDI-TOF) was performed on a Bruker Reflex III (Bruker, Breman, Germany) mass spectrometer operated in linear, positive ion mode with a N_2 laser. Laser power was used at the threshold level required to generate a signal. The accelerating voltage was set to 28 kV. Dithranol was used as the matrix and prepared as a saturated solution in THF. Allotments of the matrix and sample were thoroughly mixed together; 0.5 mL of this was spotted on the target plate and allowed to dry.

Synthesis. All manipulations were performed under an Ar or N_2 atmosphere in a glovebox or by using standard Schlenk-line techniques. All solvents were freshly distilled over an appropriate drying agent (Na or K) and degassed before use. $Mo_2(O_2C^tBu)_4$[9] and $W_2(O_2C^tBu)_4$[10] were prepared according to previously published literature procedures, and all other chemicals were purchased from industrial sources and used without further purification. $\mathbf{I}^+PF_6^-$ and $\mathbf{II}^+PF_6^-$ were generated in situ by the addition of 1 equiv of $AgPF_6$ to a THF solution of the corresponding neutral compounds.

$Mo_8(O_2C^tBu)_4(\mu$-SC_4H_2-3,4-$\{CO_2\}_2)_6$ (I). A Schlenk tube was charged with $Mo_2(O_2C^tBu)_4$ (0.600 g, 1.01 mmol) and SC_4H_2-3,4-$(CO_2H)_2$ (0.173 g, 1.00 mmol), to which toluene (15 mL) was added. The resulting yellow suspension was stirred for 21 days and the product isolated by centrifugation. The precipitate was washed with a 15-mL aliquot of toluene followed by a 15-mL aliquot of hexane before drying for 16 h in vacuo to give 0.255 g (70% yield) of a yellow microcrystalline solid. Despite extended drying times, the ^{1}H NMR spectrum of the product always shows toluene resonances, specifically 1.9 molecules of toluene per molecule of **I** in this instance. Elem anal. Calculated for $Mo_8C_{56}O_{32}S_6H_{48}\cdot(toluene)_{1.9}$: C, 35.15; H, 2.67. Found: C, 34.40; H, 2.73. ^{1}H NMR (THF-d_8): δ 8.07 (s, 4H), 8.04 (d, $J_{HH} = 3.6$ Hz, 4H), 7.57 (d, $J_{HH} = 3.2$ Hz, 4H), 1.25 (s, 36H) ppm. MALDI-TOF: calcd monoisotopic MW for $Mo_8C_{56}O_{32}S_6H_{48}$, 2192.82 ($M^+$); found, 2192.43. UV−vis (0.237 mM in THF, 295 K, values of $\epsilon \times 10^{-3}$ are given in parentheses): 390 (34.6), 304 sh (16.4) nm.

$W_8(O_2C^tBu)_4(\mu$-SC_4H_2-3,4-$\{CO_2\}_2)_6$ (II). A Schlenk tube was charged with $W_2(O_2C^tBu)_4$ (0.500 g, 0.65 mmol) and SC_4H_2-3,4-$(CO_2H)_2$ (0.210 g, 0.64 mmol), and then toluene (15 mL) was added. The resulting suspension was stirred for 28 days, during which time a red solution and precipitate formed. The product was isolated by centrifugation, washed with 2 aliquots of toluene (15 mL) and 1 aliquot of hexane (15 mL), and dried in vacuo for 6 h to give 0.210 g (68% yield) of **II** as a red microcrystalline solid. As seen for **I**, a toluene solvate always appears in the ^{1}H NMR spectrum of the product. ^{1}H NMR (THF-d_8): δ 7.86 (s, 4H), 7.67 (d, $J_{HH} = 3.6$ Hz, 4H), 7.45 (d, $J_{HH} = 3.6$ Hz, 4H), 1.16 (s, 36H) ppm. MALDI-TOF: calcd monoisotopic MW for $W_8C_{56}O_{32}S_6H_{48}$, 2895.65 (M^+); found, 2895.84. UV−vis (0.238 mM in THF, 295 K, values of $\epsilon \times 10^{-3}$ are given in parentheses): 500 (33.2), 427 sh (22.0) nm.

Electronic Structure Calculations. Electronic structure calculations employing density functional theory were performed on the model compounds $M_8(O_2CH)_4(\mu$-SC_4H_2-3,4-$\{CO_2\}_2)_6$ [M = Mo (**I***); M = W (**II***)] with the aid of the *Gaussian03* suite of programs.[11] The B3LYP functional[12] and 6-31G* basis set[13] were used for H, C, and O, and the 6-31+G(2d) basis set was used for S, along with the SDD energy-consistent pseudopotentials for Mo

(7) Byrnes, M. J.; Chisholm, M. H.; Clark, R. J. H.; Gallucci, J. C.; Hadad, C. M.; Patmore, N. J. *Inorg. Chem.* **2004**, *43*, 6334.
(8) Chisholm, M. H.; Epstein, A. J.; Gallucci, J. C.; Feil, F.; Pirkle, W. *Angew. Chem., Int. Ed.* **2005**, *44*, 6537.
(9) Brignole, A. B.; Cotton, F. A. *Inorg. Synth.* **1971**, *13*, 81.
(10) Santure, D. J.; Huffman, J. C.; Sattelberger, A. P. *Inorg. Chem.* **1985**, *24*, 371.
(11) Frisch, M. J.; et al. *Gaussian03*, revision B.04; Gaussian, Inc.: Pittsburgh, PA, 2003.
(12) (a) Lee, C.; Yang, W.; Parr, R. G. *Phys. Rev. B: Condens. Matter* **1988**, *37*, 785. (b) Becke, A. D. *Phys. Rev. A* **1988**, *38*, 3098. (c) Becke, A. D. *J. Chem. Phys.* **1993**, *98*, 5648.
(13) Hehre, W. J.; Radom, L.; Schleyer, P. v. R.; Pople, J. A. *Ab initio Molecular Orbital Theory*; John Wiley & Sons: New York, 1986.

Table 1. Single-Crystal X-ray Data for **I**

empirical formula	$C_{56}H_{48}Mo_8O_{32}S_6$
fw	2192.82
temp (K)	150(2)
wavelength (Å)	0.710 73
cryst syst	tetragonal
space group	$I4_1/a$
a (Å)	15.315(2)
b (Å)	15.315(2)
c (Å)	39.624(7)
α (deg)	90
β (deg)	90
γ (deg)	90
V (Å^3)	9294(2)
Z	4
d_{calc} (Mg m^{-3})	1.567
abs coeff (mm^{-1})	1.244
F(000)	4288
cryst size (mm^3)	0.31 × 0.27 × 0.19
θ range for data collection (deg)	2.06−27.51
index ranges	$-19 \le h \le 19$, $-14 \le k \le 14$, $-51 \le l \le 45$
reflns collected	43 988
independent reflns	5336 ($R_{int} = 0.046$)
reflns obsd ($>2\sigma$)	3930
data completeness	0.997
refinement method	full-matrix least squares on F^2
data/restraints/param	5336/6/229
GOF on F^2 [a]	1.168 [1.052]
final R indices [$I > 2\sigma(I)$][a]	R1 = 0.0506 [0.0652], wR2 = 0.1444 [0.1870]
R indices (all data)[a]	R1 = 0.0684 [0.0892], wR2 = 0.1544 [0.2107]
largest diff peak and hole (e Å^{-3})[a]	1.346 and −1.041 [1.678 and −1.186]

[a] Statistics prior to the treatment of data with the SQUEEZE subroutine of PLATON are bracketed.

and W.[14] Geometries were optimized at the above levels of theory in S_4 symmetry using the default optimization criteria of the program and confirmed local minima on the potential energy surfaces using frequency analysis.

X-ray Crystallography. The data collection crystal for $Mo_8(O_2C^tBu)_4(\mu\text{-}SC_4H_2\text{-}3,4\text{-}\{CO_2\}_2)_6$ was a yellow multifaceted chunk. Examination of the diffraction pattern on a Nonius Kappa CCD diffractometer indicated a tetragonal crystal system, and the data collection was set up to measure an octant of reciprocal space with a redundancy factor of 4.3, which means that 90% of the reflections were measured at least 4.3 times. All work was done at 150 K using an Oxford Cryostream Cooler. A combination of φ and ω scans with a frame width of 1.0° was used. Data integration was done with Denzo, and scaling and merging of the data were done with Scalepack.[15] The structure was solved in $I4_1/a$ using direct methods in SHELXS-97,[16] and full-matrix least-squares refinements based on F^2 were performed in SHELXL-97[17] with the aid of the WinGX suite of programs.[18] All hydrogens were included in the model at calculated positions using a riding model with $U(H) = 1.5U_{eq}$ (bonded carbon atom) for methyl hydrogens and $U(H) = 1.2U_{eq}$ (bonded carbon atom) for the thienyl hydrogens. The ^{t}Bu methyl groups are rotationally disordered and were modeled as two isotropic sets of atoms.

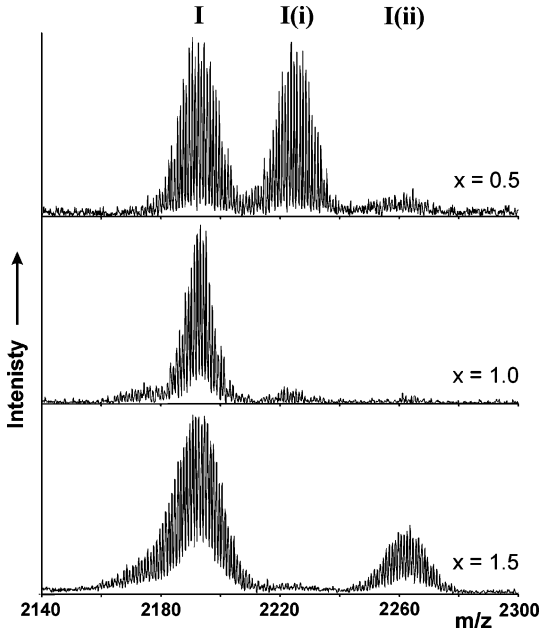

Figure 1. MALDI-TOF of the product mixtures from the reactions between $Mo_2(O_2C^tBu)_4$ and $x(SC_4H_2\text{-}3,4\text{-}\{CO_2H\}_2)$, where $x = 0.5$, 1.0, and 1.5. The intermediates $Mo_8(O_2C^tBu)_6(SC_4H_2\text{-}3,4\text{-}\{CO_2\}_2)_5$ and $Mo_8(O_2C^tBu)_8(SC_4H_2\text{-}3,4\text{-}\{CO_2\}_2)_4$ are labeled as **I(i)** and **I(ii)**, respecctively.

The structure contains voids (676 Å^3) comprised of disordered solvent molecules that could not be effectively modeled and are responsible for the elevated residuals reported. By symmetry, there are four such regions in the unit cell. The data were subjected to the SQUEEZE subroutine of PLATON,[19] to remove this contribution of electron density from the intensity data. The experimental data related to the structure determination, shown in Table 1, contain information before and after the structure has been SQUEEZED.

Results and Discussion

The reactions between $M_2(O_2C^tBu)_4$ compounds (M = Mo or W) and 3,4-thienyldicarboxylic acid were carried out in toluene at room temperature and monitored with time over a period of 21 days. By ^{1}H NMR and mass spectrometry (MALDI), we observed the formation of a series of compounds, leading to $M_8(O_2C^tBu)_8(\mu\text{-}SC_4H_2\text{-}3,4\text{-}\{CO_2\}_2)_4$, $M_8(O_2C^tBu)_6(\mu\text{-}SC_4H_2\text{-}3,4\text{-}\{CO_2\}_2)_5$, and ultimately $M_8(O_2C^tBu)_4(\mu\text{-}SC_4H_2\text{-}3,4\text{-}\{CO_2\}_2)_6$. The compounds $M_8(O_2C^tBu)_4(C_4H_2S\text{-}3,4\text{-}\{CO_2\}_2)_6$, **I** (M = Mo) and **II** (M = W), thus represent thermodynamically favored compounds in the reaction shown in eq 1 and are formed irrespective of the relative concentration of the 3,4-thienylcarboxylic acid in the range of 0.5−1.5 equiv, although 1 equiv gave the cleanest product mixture. See Figure 1. The absence of smaller aggregates testifies to the kinetic facility of carboxylate group exchange. The products **I** and **II** formed in eq 1 are obtained as microcrystalline materials that are sparingly soluble in toluene. The yellow compound **I** and red compound **II** are highly air-sensitive and must be handled in dry- and oxygen-free inert atmospheres and solvents.

(14) Andrae, D.; Haeussermann, U.; Dolg, M.; Stoll, H.; Preuss, H. *Theor. Chim. Acta* **1990**, *77*, 123.
(15) Otwinowski, Z.; Minor, W. Macromolecular Crystallography. In *Methods in Enzymology*; Carter, C. W., Jr., Sweet, R. M., Eds.; Academic Press: New York, 1997; Vol. 276, Part A, pp 307−326.
(16) Sheldrick, G. M. *Acta Crystallogr., Sect. A* **1990**, *46*, 467.
(17) Sheldrick, G. M. *SHELXL-97*; Universität Göttingen: Göttingen, Germany, 1997.
(18) Farrugia, L. J. *J. Appl. Crystallogr.* **1999**, *32*, 837.
(19) Spek, A. L. *J. Appl. Crystallogr.* **2003**, *36*, 7.

$$M_2(O_2C^tBu)_4 + SC_4H_2\text{-}3,4\text{-}(CO_2H)_2 \rightleftharpoons \text{(Unidentified intermediates)} \quad (1)$$

$$M_8(O_2C^tBu)_8(SC_4H_2\text{-}3,4\text{-}\{CO_2\}_2)_4 \xrightleftharpoons{+2HO_2C^tBu,\ +SC_4H_2\text{-}3,4\text{-}(CO_2H)_2} M_8(O_2C^tBu)_6(SC_4H_2\text{-}3,4\text{-}\{CO_2\}_2)_5 \xrightleftharpoons{+2HO_2C^tBu,\ +SC_4H_2\text{-}3,4\text{-}(CO_2H)_2} M_8(O_2C^tBu)_4(SC_4H_2\text{-}3,4\text{-}\{CO_2\}_2)_6$$

^{1}H NMR Spectra. The ^{1}H NMR spectrum of **I** in THF-d_8 is shown in Figure 2, and that of **II** is given in the Supporting Information. There is only one type of pivalate group, but there are two types of thienyldicarboxylates in the integral ratio 2:1. The ^{1}H NMR data are entirely consistent with a chain of four Mo_2 units linked by thienylcarboxylate groups or by a polyhedral arrangement of the type shown in Chart 1. It is difficult to reconcile a chain structure involving four Mo_2 units as being uniquely favored with respect to a chain of three or five M_2 units. A polygon involving the ultimate and stepwise formation of a pseudotetrahedral-like $[M_2L]_4(\text{bridge})_6$ structure is more appealing. Furthermore, in such a structure, one might anticipate that intramolecular O···M_2 bonding along the MM axis might act as a templating force. These intermolecular O···M_2 bonding motifs are commonly seen in solid-state structures of $M_2(O_2CR)_4$ compounds.

Solid-State and Molecular Structures. Crystals of **I** were obtained by slow evaporation of a 4:1 toluene/THF mixture, and the structure was solved in the tetragonal space group $I4_1/a$. The unit cell contains four Mo_8 polygons, but each polygon is situated around a $\bar{4}$ special position and hence

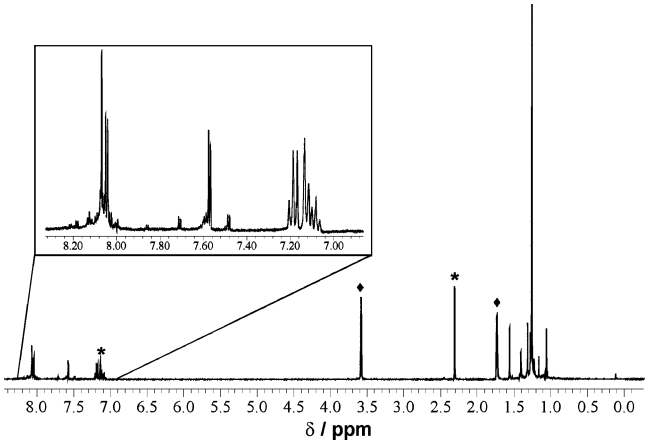

Figure 2. ^{1}H NMR spectrum of **I** in THF-d_8 with an expansion of the aromatic region. Residual protio peaks in THF-d_8 are indicated with ◆, and toluene solvate resonances are indicated with *.

Chart 1

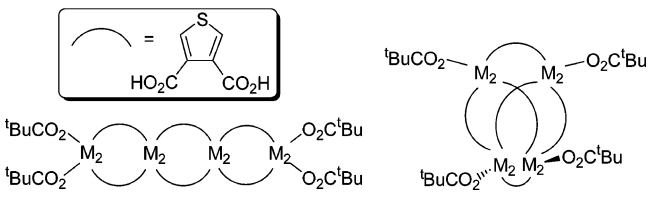

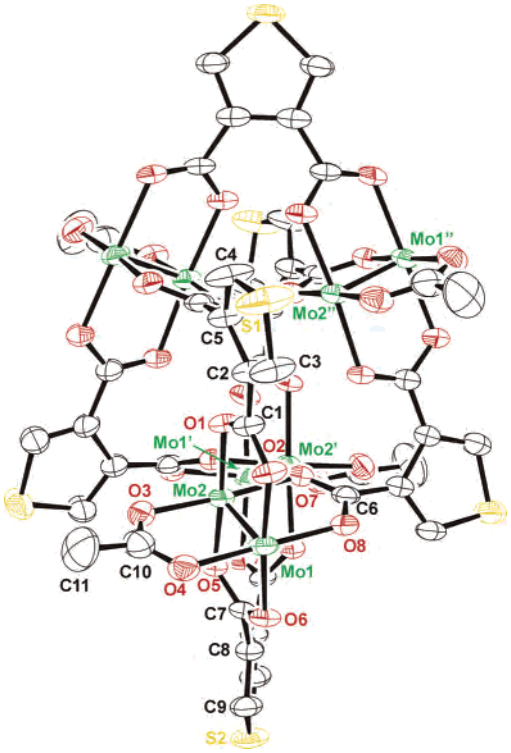

Figure 3. ORTEP diagram of **I** with the anisotropic displacement parameters drawn at the 50% probability level. The ^{t}Bu methyl groups and all hydrogen atoms have been omitted for clarity.

the asymmetric unit consists of only one-quarter of the polygon, which itself has crystallographically imposed S_4 symmetry. In the solid state, each Mo_8 unit is linked to neighboring units through intermolecular Mo···O interactions [2.920(3) Å] so as to form two one-dimensional chains of Mo_8 units, which are at right angles to one another; one is propagated along the *a* axis and the other along the *b* axis. A drawing of the unit cell is given in the Supporting Information. Within the unit cell, there are voids in which disordered solvent molecules are present (see the Experimental Section).

The molecular structure of **I** is shown in Figure 3, where it can be seen that there are two types of thienyldicarboxylate bridges, which can be termed apical (C7−C9 and S2) and meridial (C1−C5 and S1). The two apical bridges bring two Mo_2 units into close proximity with a Mo2···Mo2′ nonbonding distance of 3.8903(5) Å. Each of the adjacent Mo atoms forms intramolecular Mo···O bonds with neighboring meridial thienylcarboxylate oxygen atoms: Mo2···O7′ = 2.582(3) Å. This contact is shorter than is typically seen in the laddered structures of $Mo_2(O_2CR)_4$ compounds, Mo···O ∼ 2.9 Å.[20] For the apical thienyldicarboxylates, the O5−C7−C8−C8′ torsion angle is 33.4(6)°, which, in principle, allows electronic coupling from one Mo_2 unit to its closest neighbor via the thienyl ring. In contrast, the meridial thienyldicarboxylates have one O_2C-C_4S ring dihedral angle that is close to 0° (i.e., planar), while the other is 60°. The meridial thienyl bridges connect two $[Mo_2]_4$ units with longer Mo-to-Mo nonbonded distances, Mo2···Mo2″ = 5.5400(5)

(20) (a) Cotton, F. A.; Extine, M.; Gage, L. D. *Inorg. Chem.* **1978**, *17*, 172. (b) Martin, D. S.; Huang, H.-W. *Inorg. Chem.* **1990**, *29*, 3674.

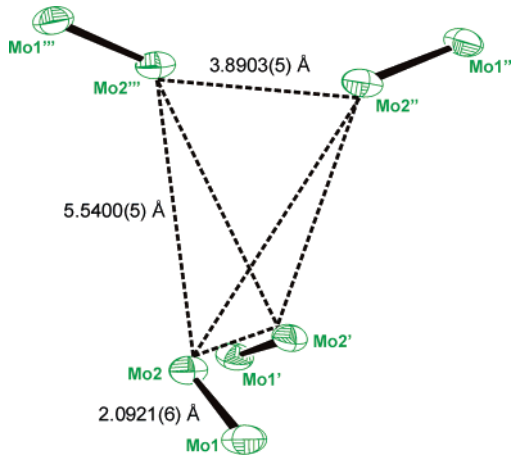

Figure 4. Diagram highlighting the bisphenoidal spatial relationship of the Mo_2 units in the crystal structure of **I**, including pertinent metric parameters.

Table 2. Selected Bond Lengths (Å), Angles (deg), and Torsion Angles (deg) for **I**, alongside Those Calculated for **I*** (See Figure 3 for Atomic Labeling Scheme)

	I	**I***
Mo1−Mo2	2.0921(6)	2.126
Mo2···Mo2′	3.8903(5)	3.882
Mo2···Mo2″	5.5400(5)	5.585
Mo2···O7′	2.582(3)	2.620
Mo2−O1	2.077(3)	2.089
Mo2−O3	2.080(3)	2.116
Mo2−O5	2.102(3)	2.102
Mo2−O7	2.160(3)	2.179
Mo1−O2	2.107(3)	2.120
Mo1−O4	2.103(3)	2.118
Mo1−O6	2.143(3)	2.150
Mo1−O8	2.101(3)	2.115
C1−C2	1.477(6)	1.471
C6−C5″	1.460(7)	1.492
C7−C8	1.482(6)	1.484
O1−C1−C2	118.8(4)	118.4
O6−C7−C8	121.6(4)	121.8
O5−C7−C8−C8′	33.4(6)	32.6
O1−C1−C2−C5	1.2(7)	1.7
O7−C6−C5″−C2″	59.6(7)	57.1

Å. The bisphenoidal arrangement of the Mo_2 units in the cluster is highlighted in Figure 4. The Mo−Mo distance is 2.0921(6) Å, and the Mo−O distances are 2.11 Å (average), which are in keeping with expectations for a $Mo_2(O_2CR)_4$ paddlewheel molecule.[21] Metric parameters for **I** are given in Table 2.

Electrochemical Studies. In a THF solution, compounds **I** and **II** each show four quasi-reversible oxidation waves in their cyclic voltammograms, as shown in Figure 5. The electrochemical potentials are given in Table 3. As expected, the tungsten complex **II** is more readily oxidized than the molybdenum analogue (by ca. 0.5 V), but perhaps most notable is the fact that the differences between oxidation potentials $\mathbf{I}/\mathbf{I}^+$, $\mathbf{I}^+/\mathbf{I}^{2+}$, $\mathbf{I}^{2+}/\mathbf{I}^{3+}$, and $\mathbf{I}^{3+}/\mathbf{I}^{4+}$ are rather similar to those of $\mathbf{II}/\mathbf{II}^+$, $\mathbf{II}^+/\mathbf{II}^{2+}$, $\mathbf{II}^{2+}/\mathbf{II}^{3+}$, and $\mathbf{II}^{3+}/\mathbf{II}^{4+}$. This provides evidence that these redox processes involve M_2 units that are not extensively coupled in an electronic sense but rather reflect electrostatic effects. For a comparison, we note

(21) Cotton, F. A.; Walton, R. A. *Multiple Bonds between Metal Atoms*, 2nd ed.; Oxford University Press: Oxford, U.K., 1993.

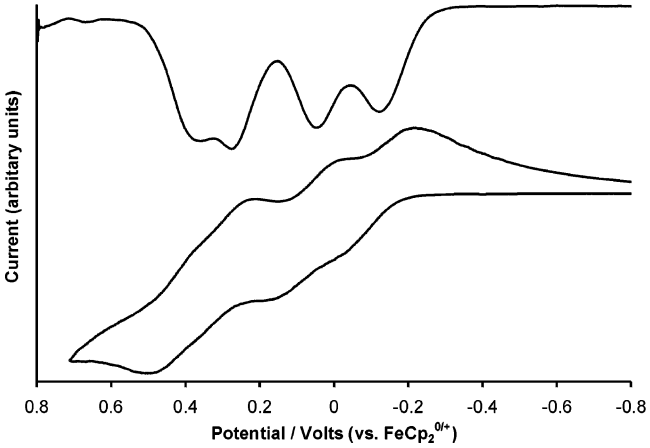

Figure 5. Cyclic voltammogram (bottom) and differential pulse voltammogram (top) of **I** in a 0.1 M $^nBu_4NPF_6$/THF solution.

Table 3. Electrochemical Oxidation Potentials for **I** and **II**, Referenced to the $FeCp_2^{0/+}$ Couple

compound	$E_{1/2}^1$ (V)	$E_{1/2}^2$ (V)	$E_{1/2}^3$ (V)	$E_{1/2}^4$ (V)
I	−0.120	0.050	0.278	0.382
II	−0.804	−0.608	−0.488	−0.410

Scheme 1

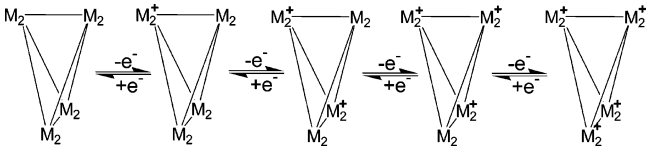

that, in the oxalate-bridged compounds $[(^tBuCO_2)_3M_2]_2(\mu\text{-}O_2CCO_2)$, the differences between the first and second oxidation waves are 717 mV for M = W and 280 mV for M = Mo.[22] Here the two M_2 centered are strongly coupled via the π system of the oxalate bridge, and the radical cations show class III behavior.[23] Particularly pertinent is a comparison with the $[(^tBuCO_2)_3M_2]_2(\mu\text{-thienyl-2,5-}\{CO_2\}_2)$ having $\Delta E_{1/2}$ = 110 mV (M = Mo) and 310 mV (M = W), which based on the EPR spectra of the radical cations represents class II and III behavior, respectively.[7,24] In contrast, Cotton has shown that when two Mo_2^{4+} units are linked by a $M(OMe)_4^{2-}$ ion, the $\Delta E_{1/2}$ values are 212 mV (M = Zn) and 207 mV (M = Co), and here the single-oxidized species has been shown to be valence trapped by both crystallography and EPR spectroscopy.[25] In the case of compounds **I** and **II**, it is interesting to speculate on the origin of the oxidation waves. Given that the structure reveals two short Mo_2···Mo_2 distances (∼3.9 Å) and four longer Mo_2···Mo_2 distances (∼5.5 Å) (see Figure 4), we imagine that oxidation proceeds in the manner shown in Scheme 1.

EPR Spectroscopy. Consistent with the view that the electronic coupling between the M_2 centers is largely electrostatic in origin is the observation that the EPR spectrum of $\mathbf{I}^+$ in THF (generated in situ by the reaction between $AgPF_6$

(22) Cayton, R. H.; Chisholm, M. H.; Huffman, J. C.; Lobkovsky, E. B. *J. Am. Chem. Soc.* **1991**, *113*, 8709.
(23) Chisholm, M. H.; Pate, B. D.; Wilson, P. J.; Zaleski, J. M. *Chem. Commun.* **2002**, 1084.
(24) Byrnes, M. J.; Chisholm, M. H. *Chem. Commun.* **2002**, 2040.
(25) Cotton, F. A.; Dalal, N. S.; Liu, C. Y.; Murillo, C. A.; North, J. M.; Wang, X. *J. Am. Chem. Soc.* **2003**, *125*, 12945.

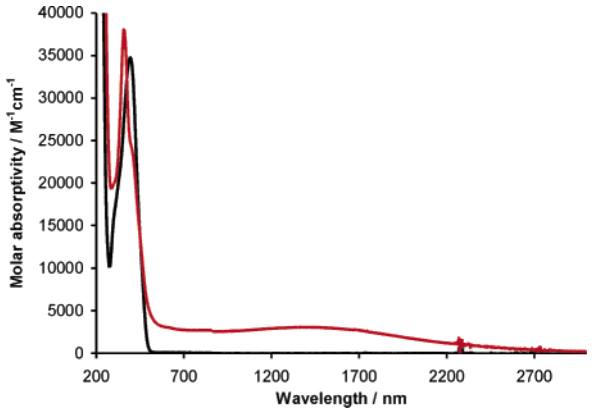

Figure 6. Electronic absorption spectrum of **I** (black) and $\mathbf{II}^{+}PF_6^{-}$ (red) in THF at 298 K.

and **I**) is comparable to that of $Mo_2(O_2C^tBu)_4^+$ with $g_0 = 1.944$ and $A_0 = 27.8$ G.[26] A similar situation is observed for $\mathbf{II}^+$, which has an EPR spectrum consistent with that of the single electron being delocalized on a single W_2^{5+} unit ($g_0 = 1.818$, $A_0 = 58.0$ G).

Electronic Absorption Spectra. The neutral complexes **I** and **II** show intense absorptions in the visible region, $\lambda_{max} = 390$ nm (**I**) and 500 nm (**II**) with $\epsilon \sim 30\,000$ M^{-1} cm^{-1}. These absorptions are at notably shorter wavelengths in relation to those of 2,5-thienyldicarboxylate-bridged M_4-containing compounds and are assignable to M_2 δ-to-thienylcarboxylate charge transfer.[7]

Upon oxidation to $\mathbf{I}^+$, a low-energy, weak, and very broad electronic absorption band is seen in the near-IR. The spectra of **I** and $\mathbf{I}^+$ are compared in Figure 6. This low-energy band can be classified as an intervalence charge-transfer (IVCT) absorption of a class II, weakly coupled system.[27] This most likely reflects electronic coupling between the Mo_2 centers that are linked by the apical thienyldicarboxylate bridge, which have the shorter Mo_2-Mo_2 distances of 3.8 Å. For reasons that are unknown to us, we have not seen a related IVCT band for $\mathbf{II}^+$.

Electronic Structure Calculations. With the aim of examining possible electronic coupling between the M_2 units in **I** and **II**, we have undertaken electronic structure calculations employing density functional theory with the aid of the *Gaussian03* suite of programs[11] on the model compounds $M_8(O_2CH)_4(SC_4H_2\text{-}3,4\text{-}\{CO_2\}_2)_6$, where M = Mo (**I***) and M = W (**II***), with both geometries optimized in S_4 symmetry. The metric parameters for **I*** are included in Table 2, where a good correlation between the calculated gas-phase (**I***) and observed solid-state (**I**) geometries is observed.

The frontier orbitals of the molecules **I*** and **II*** consist of sets of occupied M_2 δ combinations (HOMO, -1, -2, and -3) and M_2 π combinations, with the LUMO through LUMO +7 being thienylcarboxylate π^* orbitals. Most important in a consideration of electronic coupling between M_2 centers is the energy separation between the M_2 δ combinations, which arises as a result of mixing with the π^* orbitals of the bridging ligands.[28] For **II***, the splitting of W_2 δ combinations is 0.24 eV, while for **I***, the splitting of Mo_2 δ combinations is 0.16 eV. These are smaller in magnitude when compared to M_2 centers linked by 2,5-thienylcarboxylates and related strongly coupled M_2-bridge$-M_2$ centers where the M_2 δ splittings are on the order of 0.6 eV for M = W and 0.4 eV for M = Mo.[7,29] Thus, the calculations support the view that the M_2 centers are relatively weakly coupled in the complexes $\mathbf{I}^+$ and $\mathbf{II}^+$.

Concluding Remarks

The synthesis of these new MOPs by the reactions shown in eq 1 is aided by the templating effects of the 3,4-thienylcarboxylate bridge and intramolecular $Mo_2\cdots O$ bonding. These electrostatic interactions provide a thermodynamic driving force toward the final $[M_2]_4$ product, and we can anticipate that related and extended bridges could yield similar structures. The $[M_2]_4$ units show interesting electrochemistry for a system that is only weakly coupled in a molecular orbital sense. The proximity of the M_2 centers serves to bring about significant electrostatic effects in the redox processes, and these are seen to be similar for both **I** and **II**, in contrast to strongly coupled systems, where the $\Delta E_{1/2}$ values for tungsten are always significantly greater than those for molybdenum. This work illustrates the importance of incorporating M$\cdots$O electrostatic interactions as templating effects in the design of MOPs incorporating M_2 quadruply bonded units. Finally, it should be noted that mononuclear analogues of the form M4L6, and having S_4 symmetry, have been reported.[30] The present work supports the notion that "anything one can do, two can do, too—and it is more interesting".[31]

Acknowledgment. We are grateful for support of this research by grants from the National Science Foundation. Dr. Judith Gallucci is thanked for assistance in obtaining the single-crystal structure of **I**, and Dr. Kari Green-Church at the OSU Campus Chemical Instrument Center is thanked for assistance in obtaining the MALDI mass spectrometry data. The Ohio Supercomputer Center is gratefully acknowledged for generous allocation of computing time, and Dr. Christopher Hadad is thanked for computational assistance.

Supporting Information Available: Tables of metrics for non-SQUEEZED and SQUEEZED structures of **I**, including related CIF files, a crystal packing diagram for **I**, the ^1H NMR spectrum of **II**, and atomic coordinates for **I*** and **II***. This material is available free of charge via the Internet at http://pubs.acs.org.

IC051516S

(26) Chisholm, M. H.; D'Acchioli, J. S.; Pate, B. D.; Patmore, N. J.; Dalal, N. S.; Zipse, D. J. *Inorg. Chem.* **2005**, *44*, 1061.
(27) (a) Demadis, K. D.; Hartshorn, C. M.; Meyer, T. J. *Chem. Rev.* **2001**, *101*, 2655. (b) Brunschwig, B. S.; Creutz, C.; Sutin, N. *Chem. Soc. Rev.* **2002**, *31*, 168.
(28) Chisholm, M. H.; Clark, R. J. H.; Gallucci, J. C.; Hadad, C. M.; Patmore, N. J. *J. Am. Chem. Soc.* **2004**, *126*, 8303.
(29) Bursten, B. E.; Chisholm, M. H.; Clark, R. J. H.; Firth, S.; Hadad, C. M.; MacIntosh, A. M.; Wilson, P. J.; Woodward, P. M.; Zaleski, J. M. *J. Am. Chem. Soc.* **2002**, *124*, 3050.
(30) (a) Clegg, J. K.; Lindoy, L. F.; Moubaraki, B.; Murray, K. S.; McMurtrie, J. C. *Dalton Trans.* **2004**, 2417. (b) Beissel, T.; Powers, R. E.; Raymond, K. N. *Angew. Chem., Int. Ed. Engl.* **1996**, *35*, 1084.
(31) Chisholm, M. H. *ACS Symp. Ser.* **1981**, *155*, 17.